640 × 512 Pixels Long-Wavelength Infrared (LWIR) Quantum-Dot Infrared Photodetector (QDIP) Imaging Focal Plane Array

Sarath D. Gunapala, Sumith V. Bandara, Cory J. Hill, David Z. Ting, John K. Liu, Sir B. Rafol, Edward R. Blazejewski, Jason M. Mumolo, Sam A. Keo, Sanjay Krishna, Y.-C. Chang, and Craig A. Shott

***Abstract*—Epitaxially grown self-assembled InAs–InGaAs–GaAs quantum dots (QDs) are exploited for the development of large-format long-wavelength infrared focal plane arrays (FPAs). The dot-in-a-well (DWELL) structures were experimentally shown to absorb both 45° and normal incident light, therefore, a reflection grating structure was used to enhance the quantum efficiency. The devices exhibit peak responsivity out to 8.1 μm, with peak detectivity reaching $\sim 1 \times 10^{10}$ Jones at 77 K. The devices were fabricated into the first long-wavelength 640×512 pixel QD infrared photodetector imaging FPA, which has produced excellent infrared imagery with noise equivalent temperature difference of 40 mK at 60-K operating temperature.**

***Index Terms*—Focal plane array, infrared detector, quantum dots (QDs).**

I. Introduction

THE ARTIFICIAL atom-like properties of epitaxially self-assembled quantum dots (QDs) were exploited in this work for the development of large-format, long-wavelength infrared (LWIR) focal plane arrays (FPAs) with high operability and spatial uniformity. QDs are nanometer-scale islands that form spontaneously on a semiconductor substrate due to lattice mismatch. QD infrared photodetectors (QDIPs) with properly engineered dots have been predicted theoretically to have significant advantages over quantum-well infrared detectors (QWIPs) [1]–[8]. QDIPs are fabricated using robust wide bandgap III–V materials which are well suited to the production of highly uniform LWIR arrays. QD-based infrared photodetectors have the potential to make a significant impact on the next generation of infrared imaging systems. QDIPs possess all of the advantages of traditional III–V-based infrared photodetectors, such as: extremely high operability, mature fabrication technology, very large formats, and material production that is increasingly high volume and low cost. The addition of active nanoscale particles (i.e., QDs) embedded within the III–V infrared detector allows for higher operating temperatures and increased bandgap tunability without sacrificing the economic advantages of the mature III–V infrared imaging system pipeline.

The main benefit in using the QD approach stems from 3-D quantum confinement, which 1) enables normal incidence absorption by modifying the optical transition selection rule and 2) increases the photo-excited carrier lifetime by reducing optical phonon scattering via the "phonon bottleneck" mechanism [1]–[6]. However, QDs also have some drawbacks that need to be addressed. In a typical detector structure, QD densities are low (compared to the number of dopants in the active regions of QWIPs); so while individual QDs are efficient absorbers, typical QD densities are not high enough to achieve high quantum efficiency. Thus, while QD-based infrared detectors have clearly demonstrated normal incidence absorption [5], [6], and, in some instances, higher operating temperature as well [5]–[12], they are still lacking in quantum efficiency and responsivity.

II. Dot-in-the-Well (DWELL) Infrared Photodetector

The first-generation QDIPs are high-gain low-quantum-efficiency devices. Improving quantum efficiency is a key to achieving a competitive QD-based FPA technology. This can be accomplished by increasing the QD density, or by enhancing the infrared absorption in the QD-containing material. There are various versions of QDIPs, based on different materials and designs. Thus, application engineers have a choice of devices to select from for their applications. The particular application which we are interested in is remote sensing of planetary atmospheres. The tailorability of the FPA cut-off wavelength is important in this application. We chose the dot-in-a-well (DWELL) QDIP device structure shown in Fig. 1 for the ease of wavelength tunability (see Fig. 2). Our specific implementation uses InAs QDs embedded in InGaAs–GaAs multiple QW (MQW) structures, as illustrated in Fig. 1. It has been shown that this material system can support a large number of QD stacks without suffering material degradation, thereby allowing high dot density. The host InGaAs–GaAs MQW structures are highly compatible with the mature FPA fabrication process that are used routinely to make QWIP FPAs. Similar to other intersubband detectors, DWELLs operate by the photoexcitation of electrons between energy levels in the potential well created by the nanoscale QD in a well structure. The right panel of Fig. 1

Manuscript received July 6, 2006; revised October 27, 2006. The research described in this paper was performed by the Jet Propulsion Laboratory, California Institute of Technology, Pasadena, CA.

S. D. Gunapala, S. V. Bandara, C. J. Hill, D. Z.-Y Ting, J. K. Liu, E. R. Blazejewski, J. M. Mumolo, S. A. Keo, and Y.-C. Chang are with the Jet Propulsion Laboratory, California Institute of Technology, Pasadena, CA 91109 USA. (e-mail: Sarath.d.Gunapala@jpl.nasa.gov).

Y.-C. Chang is with the Department of Physics, University of Illinois at Urbana-Champaign, Urbana, IL 61801 USA.

S. B. Rafol is with the Infravision Systems, Altadena, CA 91001 USA.

S. Krishna is with the University of New Mexico, Albuquerque, NM 87106 USA.

C. A. Shott is with the FLIR Systems Inc., Indigo Operations, Goleta, CA 93117 USA.

Color versions of one or more figures in this paper are available online at http://ieeexplore.ieee.org.

Digital Object Identifier 10.1109/JQE.2006.889645

0018-9197/$25.00 © 2007 IEEE

Authorized licensed use limited to: IEEE Xplore. Downloaded on November 24, 2008 at 11:15 from IEEE Xplore. Restrictions apply.

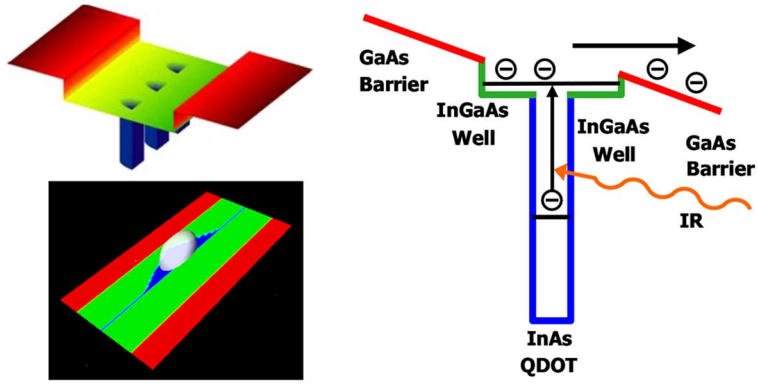

Fig. 1. Illustration of the DWELL device. Top left panel shows the potential profile, with three pyramid shaped dots embedded in the QW. The bottom left panel displays a calculated DWELL ground state wave function, represented by a white translucent equal-probability isosurface, localized by a pyramidal QD. The right panel illustrates the operation of a DWELL infrared detector.

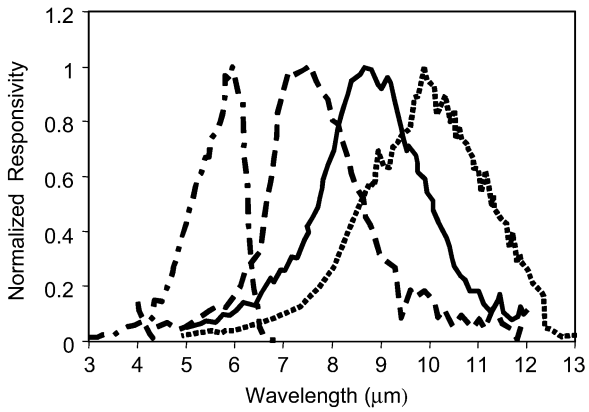

Fig. 2. Experimentally measured spectral responsivity of DWELL QDIPs demonstrating spectral tunability by varying the well width from 55 to 100 Å.

shows that, under an applied bias voltage, these photo-excited carriers can escape from the potential wells and be collected as photocurrent. The wavelengths of the spectral peaks (λ_p) are determined by the energy difference between quantized states in the DWELL. The hybrid QD/QW or DWELL, device offers two advantages: 1) challenges in wavelength tuning through dot-size control can be compensated in part by engineering the QW sizes, which can be controlled precisely and 2) QWs can trap electrons and aid in carrier capture by QDs, thereby facilitating ground state refilling [10], [11], [13]. The advantage is that it would increase the absorption quantum efficiency. But on the other hand, DWELL QDIPs have lower gain than conventional QDIPs due to carrier trapping by the QWs. In traditional QDIPs, the large photoconductive gain could lead to higher operating temperature due to the lowering of dark current. The tradeoff for DWELL QDIPs is the sacrifice in gain for higher quantum efficiency.

III. QD Material Growth

QDs can be fabricated by taking advantage of a strain-induced transformation that happens naturally in the initial stages of epitaxial growth for lattice-mismatched materials. One highly successful method of achieving QDs is through self-organized growth in the Stranski–Krastanow growth mode [14]. Similar to QWs, these structures are fabricated by metal–organic chemical vapor depostion (MOCVD) or molecular beam epitaxy (MBE) using III–V materials (e.g., InGaAs–AlAs–GaAs–InAs). Three-dimensional islands can be formed spontaneously during strained layer epitaxy, and they exhibit fairly good uniformity in size, shape and spatial distribution. By using a smaller bandgap material (InAs) for the strained layer to form the 3-D nanostructures and a larger bandgap material for the barrier (InGaAs, GaAs, or AlGaAs), three-dimensional carrier confinement can be achieved.

Our growth procedure follows closely that for the DWELL structures reported in the literature [15]. In the sample used for the FPA demonstration, the InAs QDs were grown in the center of a 75-Å $In_{0.12}Ga_{0.88}As$ QW at a substrate temperature of 490 °C. Ground state electrons were provided to the detector by doping the InAs with Si to a density of 5×10^{17} cm^{-3}. The approximate dot density is 3×10^{10} cm^{-2}, as determined by AFM of uncapped layers. We note, however, the dot density of the capped layers may differ due to segregation and diffusion. The QWs were separated by 500 Å of undoped GaAs. We have increased the overall number of photosensitive DWELL stacks to 30. This has led to much higher quantum efficiency in our structures than previously reported values for DWELL QDIP structures [10]. This photosensitive DWELL structure is sandwiched between 0.66-μm GaAs top and 0.5-μm bottom contact layers doped $n = 5 \times 10^{17}$ cm^{-3}. All DWELL-QDIP wafers were grown on semi-insulating 75-mm GaAs substrates.

IV. Test Detector Fabrication

After evaluating material quality, selected wafers were processed into 200 μm × 200 μm test detector mesas. DWELL QDIP test detectors were fabricated by standard wet and dry chemical etching through the stack of photosensitive layers into the doped GaAs bottom contact layer. The top of the detectors was covered with Au–Ge and Au for an Ohmic contact, which also serves as a reflector for light incident through the bottom contact, allowing two passes through the active layers.

Initial QDIP characterization of discrete devices included measurements of the room-temperature absorption spectra, side [16], [17], and normal incident responsivity spectra, dark

Authorized licensed use limited to: IEEE Xplore. Downloaded on November 24, 2008 at 11:15 from IEEE Xplore. Restrictions apply.

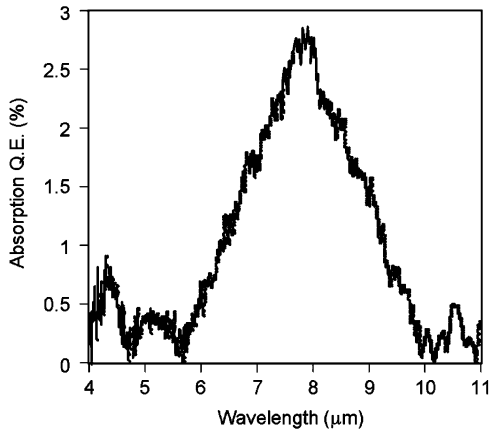

Fig. 3. Measured internal absorption quantum efficiency (no grating or cavity effects) for a 30-stack DWELL QDIP.

current, and noise. These detectors were tested in a cryogenically cooled test bed using a calibrated blackbody source to evaluate the responsivity of the detector over the relevant range of operating temperatures and bias voltages. The test results were used to verify and adjust the model used in designing the material parameters. This cycle was iterated several times in order to develop the recipe for the final optimized detector wafer used to make FPAs.

V. DWELL QDIP ABSORPTION QUANTUM EFFICIENCY

A separate 8-pass polished waveguide structure was fabricated for absorption measurements [16], [17]. Fig. 3 shows the measured absorption quantum efficiency from a 30-stack DWELL QDIP, with a peak value at approximately 2.7%. To our knowledge, this is the highest measured intrinsic absorption quantum efficiency published to date in a QD-based LWIR infrared detector. A typical set of results on measured normal and 45-deg incidence responsivity of the DWELL QDIP samples are shown in Fig. 4. It is found that the normal incidence responsivity (relative to the 45-deg responsivity) is much stronger (almost 1 order of magnitude) than that for the typical QWIP. At the same time, we also find that the 45-deg incidence responsivity is four to five times stronger than the normal incidence responsivity. This observation is consistent with our simulation results [18]. In the typical InAs–(In)GaAs QDIP, the dot base width is much larger than the dot height. In such low-aspect-ratio dots, while the ground to the first excited state transition can produce strong normal incidence absorption, it does not contribute appreciably to the photocurrent under small or moderate biasing conditions because the first excited state is deeply bound. Instead, the typical observed photo-response is due to transition to higher excited states, and such transitions could be induced by either normal-incidence or inclined incidence light, depending on the symmetry of the states involved in the optical transition. It should be noted that this observed property is not specific to the DWELL QDIP; similar theoretical and experimental results on conventional InAs–GaAs QDIPs have also been reported [19].

Fig. 4 indicates that at wavelength range shown, our DWELL QDIPs have reasonable absorption strength for normal-incidence light (x, y-polarized; with z being the normal incidence

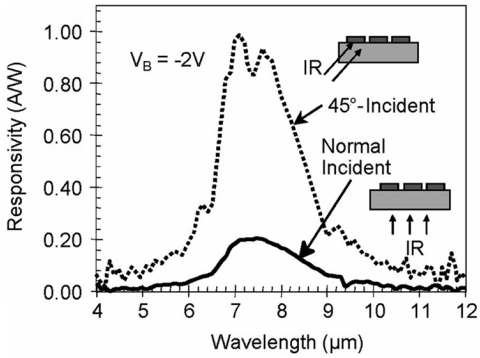

Fig. 4. DWELL QDIP spectral responsivity measured for (a) normal incidence and (b) 45° incidence.

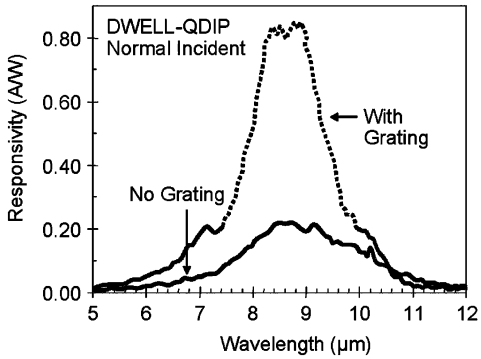

Fig. 5. Normal incidence spectral responsivity of a DWELL-QDIP with and without reflection gratings.

direction), but also absorbs inclined (or side) incidence (z-polarized) light even more strongly. Accordingly, we designed a reflection grating structure to take advantage of the detector's ability to absorb both normal and inclined incidence light in order to maximize quantum efficiency. As in QWIPs, normal incidence light can be coupled to the z-polarization light absorption mechanism in DWELL QDIPs by using a reflection grating. For this experiment we grew a separate sample, with a slightly adjusted well structure. Fig. 5 shows our measured results on grating enhancement. Normal incidence responsivity was measured for the DWELL QDIP sample, fabricated both with and without a reflection grating. The device with the reflection grating shows almost four times larger normal incident responsivity than the one without, clearly indicating the promise of this approach.

Given that the gain of DWELL QDIPs is quite different (typically less than 1) from other intersubband detectors, it is worthwhile to examine how this affects the detector performance. The sensitivity of DWELL QDIPs can be evaluated by measuring parameters such as absolute spectral responsitivity $R(\lambda)$, absorption quantum efficiency (internal) η, photocurrent (I_P), dark current I_D, noise current i_n, and specific detectivity $(D*)$. Similar to other intersubband photodetectors, these parameters are linked to each other through the photoconductive gain (g) of the detector, $R = e\eta g/(hc/\lambda), i_n = \sqrt{4e(I_D + I_P)g\Delta f}$, and $D* = R\sqrt{A\Delta f}/i_n$ [16], [17]. Here, e is the electron charge, Δf is the bandwidth, A is the detector area, and hc/λ is the photoexcitation energy. When the detector operates in background limited conditions ($I_P \gg I_D$), since I_P is proportional to gain,

Authorized licensed use limited to: IEEE Xplore. Downloaded on November 24, 2008 at 11:15 from IEEE Xplore. Restrictions apply.

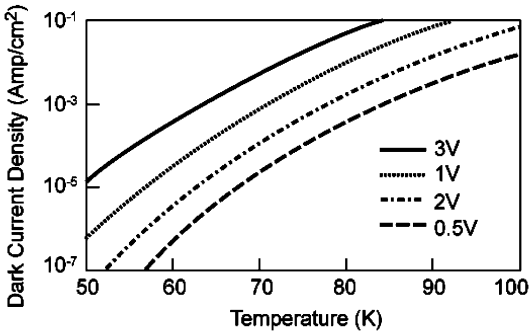

Fig. 6. Dark current density versus operating temperature curves of a DWELL QDIP detector at various device bias conditions.

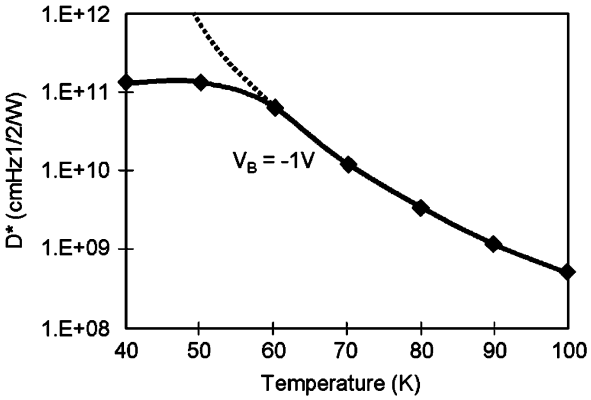

Fig. 7. Dark current limited and background (300K, f/2 optics) limited specific detectivity of DWELL-QDIP as a function of operating temperature. Dark current limited detectivities are calculated using $D* = R\sqrt{A\Delta f}/i_n$, experimentally measured spectral responsivity and noise. Background limited detectivities are calculated using the noise due to total current (i.e., experimentally measured dark current + estimated photo current due to 300K f/2 background with emissivity $e = 1$ and experimentally measured responsivity).

$D*$ depends only on the absorption quantum efficiency η, regardless of the size of the photoconductive gain. Therefore, improving absorption quantum efficiency is the key to improving the ultimate performance of these detectors for background limited operation [16], [17]. Fig. 6 shows the dark current as a function of temperature at various operating bias conditions. Fig. 7 shows D^* of this detector as a function of device temperature at operating bias $V_B = -1V$. This figure shows that the DWELL detector reaching background limited $D^* \sim 1 \times 10^{11}$ Jones around $T = 50$ K temperature. In the future, we expect to improve D^* through reduction of dark current and increase in quantum efficiency. Specifically: 1) dark current reduction would extend the plateau of the BLIP (background limited performance) D^* curve to higher temperature; and 2) quantum efficiency increase would shift the BLIP D^* curve upward over the entire temperature range. Further reduction in dark current would help to achieve BLIP performance at higher operating temperatures.

VI. FPA Fabrication

After establishing optimized layer thickness and growth conditions for the LWIR DWELL-QDIP, the FPA material was grown on 75-mm semi-insulating GaAs substrates. Selected wafers were processed into FPAs. After the 2-D grating array was defined by photolithography and dry etching, the LWIR detector pixels of the 640×512 FPAs were fabricated by dry etching through the photosensitive GaAs–In_x Ga_{1-x} As–InAs layers into the 0.5-μm-thick doped bottom GaAs (i.e., detector common) layer. The pitch of the FPA is 25 μm, and the actual QDIP pixel size is 23×23 μm^2. The 2-D grating reflectors on top of the detectors were then covered with Au–Ge and Au for Ohmic contact and reflection. Twelve FPAs were processed on a 75 mm GaAs wafer. Indium bumps were then evaporated on top of the detectors for silicon read out integrated circuit (ROIC) hybridization. Several FPAs were chosen and hybridized (via an indium bump-bonding process) to a 640×512 pixel direct injection CMOS ROIC (ISC-9803).

After the 640×512 pixel QDIP detector arrays were hybridized to a 640×512 pixel ROIC, a simple electronic functionality test was performed to evaluate the FPAs. Then we thinned the selected FPA hybrids by removing the entire substrate while leaving the detector pixels, the bottom contact layer and the dielectric mirror. During thinning, the entire substrate material was removed by abrasive polishing, wet chemical etching followed by dry etching that ends at the epitaxially grown selective etch layer. This thinned detector array completely eliminates the thermal mismatch issue between the CMOS ROIC and the GaAs–InAs–AlAs-based detector array, pixel outages, and pixel-to-pixel optical cross talk of the FPA. Basically, the thinned GaAs-based QDIP FPA membrane adapts to the thermal expansion and contraction coefficients of the silicon ROIC. Thus, thinning has played an extremely important role in the fabrication of large area FPA hybrids. Elimination of thermal mismatch is a process of paramount importance in achieving high quality, large area FPAs without pixel delamination [16]. Another important consequence of the thinning process is that the thinned structure effectively forms a wavguide that serves to enhance the optical field, thereby increasing the absorption quantum efficiency.

VII. FPA Demonstration

Selected detector hybrids were mounted and wire-bonded to a leadless chip carrier (LCC). A specially designed dewar was used to characterize the FPA functionality using a general-purpose electronic system from SE-IR Incorporated. The SE-IR system was programmed to generate complex timing patterns, and was reconfigured to handle a development grade FPAs. The best performance was determined by optimizing operating-parameters for each FPA. The FPAs were characterized for pixel responsivity, quantum efficiency, noise, $D^*, NE\Delta T$, pixel operability, before and after uniformity correction (contribution form both spatial and temporal), and pixel operability. The spectral responsivity of the FPA was determined using a separate single mesa test device processed with the FPA. $NE\Delta T$ as a function of bias and integration time at a fixed operating temperature was used as a metric for parameter optimization.

Since the QDIP is a high impedance device at operating temperature, it should yield a very high charge injection coupling efficiency into the integration capacitor of the ROIC. Charge injection efficiency can be obtained from $E_{\text{inj}} = g_m R_D/(1 + g_m R_D)$, where g_m is the transconductance of the MOSFET obtained from the measured dark current by using the expression $g_m = eI_{\text{Det}}/\text{kT}$. The dynamic resistance R_D of the detector and

Authorized licensed use limited to: IEEE Xplore. Downloaded on November 24, 2008 at 11:15 from IEEE Xplore. Restrictions apply.

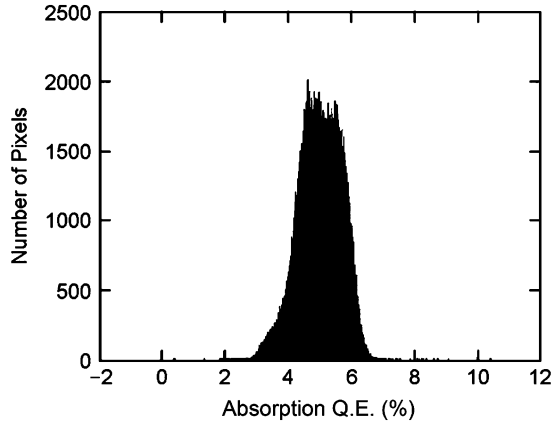

Fig. 8. Uncorrected noise equivalent temperature difference ($NE\Delta T$) histogram of the 311 040 pixels of the 640 × 512 pixel QDIP FPA. The uncorrected nonuniformity (= standard deviation/mean) of this unoptimized FPA is approximately 20%. Higher nonuniformity is attributed to the reduced number of samples collected during the experiment. The corrected nonuniformity has reduced to 0.2% after two-point correction.

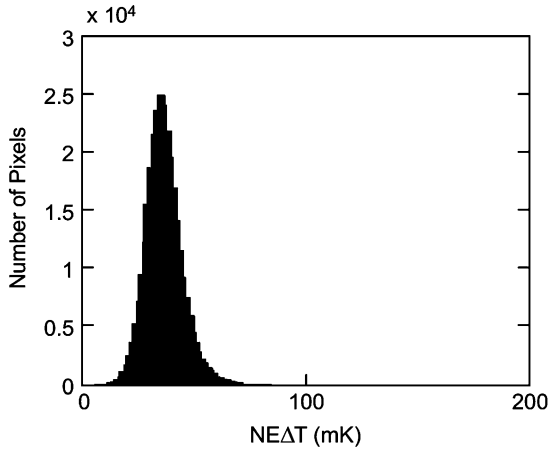

Fig. 9. Experimentally measured absorption quantum efficiency histogram of the 311 040 pixels of the 640 × 512 pixel QDIP FPA. The photoconductive gain of the detector at $V_B = -350$ mV is 0.14.

ROIC is calculated from $R_D \cdot C_{\rm ROIC} = t_{\rm int}$, where $C_{\rm ROIC}$ is the capacitance of the ROIC integration capacitor, and $t_{\rm int}$ is the integration time. The measured differential resistance $R_{\rm Det}$ of the 23×23 μm^2 pixels at -350 mV bias is 5.5×10^{10} Ω (compared to the calculated dynamic resistance of $R_D = 5.7 \times 10^{10}$ Ω) at $T = 60$ K, and detector capacitance $C_{\rm Det}$ is 1.4×10^{-14} F. The detector total current (i.e., $\rm dark + photo$) is $I_{\rm Det} = 17$ pA under the same operating conditions. We have integrated the signal for 20 ms. The input capacitance of ISC 9803 ROIC is 350 fF, which yields R_D of $5.7 \times 10^{10}\Omega$. According to the equation above, the charge injection efficiency $E_{\rm inj} = 99.65\%$ at a frame rate of 30 Hz. The FPA was back-illuminated through the flat thinned substrate membrane (thickness $E_{\rm inj} = g_m R_D/(1 + g_m R_D)$ 1000 Å). This initial array gave very good images with >99% of the pixels working, demonstrating the high yield of GaAs technology. The operability was defined as the percentage of pixels having $NE\Delta T$ within 3 σ at 300 K background with f/2 optics and in this case operability happens to be equal to the pixel yield.

We have used the following equation to calculate the FPA $NE\Delta T$: $NE\Delta T = \sqrt{AB}/[D_B^*(dP_B/dT)\sin^2(\theta/2)]$, where D_B^* is the blackbody detectivity, dP_B/dT is the derivative of the integrated blackbody power with respect to temperature, and θ is the field of view angle [i.e., $\sin^2(\theta/2) = (4f^2+1)^{-1}$, where f is the f number of the optical system]. The background temperature $T_B = 300$ K, the area of the pixel $A = (23\ \mu{\rm m})^2$, the f number of the optical system is 2, and the frame rate is 30 Hz. Fig. 8 shows the experimentally measured $NE\Delta T$ histogram of the FPA at an operating temperature of $T = 60$ K, bias $V_B = -350$ mV at 300-K background with f/2 optics. The mean $NE\Delta T$ value is 40 mK. This agrees reasonably well with our estimated value of 25 mK based on test structure data. The read noise of the multiplexer is 500 electrons. The experimentally measured FPA mean quantum efficiency of the FPA was 5.0% (See Fig. 9). Thus, the absorption quantum efficiency of the DWELL QDIP discussed in this paper has increased by a factor of 1.8 due to optical cavity/waveguiding effects resulting from substrate thinning. This is very similar to light coupling efficiency enhancement due to substrate thinning routinely obtained in QWIP FPAs. The experimentally measured photoconductive gain of the detector pixels at $V_B = -350$ mV is 0.14.

VIII. Focal Plane Array Camera

A 640×512 pixel QDIP FPA hybrid was mounted onto a 84-pin LCC and installed into a laboratory dewar which is cooled by liquid nitrogen to demonstrate a LWIR imaging camera. The FPA was cooled to 60K by pumping on liquid nitrogen and the temperature was stabilized by regulating the pressure of gaseous nitrogen. The circular cold stop of the imaging system was f/2 and the dewar window transmission was 90%. The digital data acquisition resolution of the camera is 14-bits, which determines the instantaneous dynamic range of the camera (i.e., 16 384) [16], [17].

The measured mean $NE\Delta T$ of the QDIP camera is 40 mK at an operating temperature of $T = 60$ K and bias $V_B = -350$ mV at 300 K background with f/2 optics. This is in good agreement with expected FPA sensitivity due to the practical limitations on charge handling capacity of the multiplexer, read noise, bias voltage and operating temperature. The uncorrected $NE\Delta T$ nonuniformity of the 640×512 pixels FPA is about 20% (= sigma/mean). Fig. 8 shows the $NE\Delta T$ histogram of this first unoptimized 640×512 pixel QDIP FPA and the higher sigma/mean was due to the reduced number of samples acquired during the measurement. The number of samples was reduced by a factor of 16 due to the high 1/f noise of the data acquisition system used during this experiment. The nonuniformity after two-point (17° Cand 27 ° C) correction improves to less than 0.2%. The corrected nonuniformity could be reduced if we use a measurement system with lower 1/f noise.

Video images were taken at a frame rate of 30 Hz at temperatures as high as $T = 60$ K using a ROIC capacitor having a maximum charge capacity of 11×10^6 electrons (the maximum number of photoelectrons and dark electrons that can be counted in the integration time of each detector pixel). Fig. 10 shows an image taken with this long-wavelength 640×512 pixels QDIP camera.

Authorized licensed use limited to: IEEE Xplore. Downloaded on November 24, 2008 at 11:15 from IEEE Xplore. Restrictions apply.

Fig. 10. Image taken with the first 640 × 512 pixels QDIP LWIR FPA imaging system with an f/2 AR coated germanium optical assembly.

IX. Conclusion

Rapid progress in the development of QD infrared detector technology has resulted in the demonstration of a number of MWIR and LWIR FPA in the 256 × 256 or 320256 format, operating at temperatures ranging from 80 to 135 K [20]–[22]. In this work we report a 640 × 512 pixel LWIR QDIP FPA with $NE\Delta T$ of 40 mK at an operating temperature of 60 K. To the best of our knowledge, this is the largest format LWIR QDIP FPA demonstrated to date. In addition, it also has the lowest $NE\Delta T$. A unique feature of this QDIP FPA is the use of a reflection grating to improve detection sensitivity. The higher sensitivity (i.e., low $NE\Delta T$) is attributed to the higher responsivity. This high responsivity is directly associated with the light coupling grating and optical cavity effect, without which the responsivity would have been an order of magnitude lower. We should point out that the reflection grating-based sensitivity enhancement scheme could be implemented not just for DWELL QDIPs, but for conventional QDIPs also.

The performance of DWELL-QDIP presented here still lags behind that for the state-of-the-art QWIPs. The D^* is still limited by the high dark current and the relatively low quantum efficiency. To improve the device performance, we would need to optimize the device structure to decrease the dark current, and to increase the dot density or the number of dot stacks.

In evaluating the quality of an image from a FPA, of particular interest is the role of FPA parameters such as operability and uniformity. A more detailed discussion on this subject can be found in [17], which points out that for $D^* \geq 10^{10}$ cm·Hz/W, the FPA imaging performance becomes less dependent on detectivity and more on array spatial uniformity. Although the 40-mK $NE\Delta T$ value presented in this work is best achieved to date in a QDIP-based FPA, it is also not quite as low as that for the QWIP FPAs (typically less than 20 mK). As mentioned earlier, this is in part attributed to the fewer number of samples collected during the FPA characterization. In addition, this could be attributed to the lower detectivity, and possibly also to lower spatial uniformity of the QDIP material due to size distribution of QDs. To improve $NE\Delta T$, we would need to increase the detectivty and FPA uniformity. One of the assumed advantages of QDIP is that it should produce FPAs with high spatial uniformity since it is based on mature III–V materials. Our results seem to indicate that although the spatial uniformity is not yet on par with the excellent uniformity demonstrated in QWIPs, it nevertheless is quite good for an early demonstration FPA, and hopefully should improve as QD growth technology matures. Another aspect is that since the QDIP arrays can be thinned down to a membrane, the thermal mismatch issues between detector array and silicon ROIC are eliminated. Consequently, the QDIP interconnect operability should also be quite high. The FPA performance presented in this work is significant in that it demonstrates QDIP FPAs with high operability and high spatial uniformity could be attainable in practice.

Finally, it should be noted that in addition to the performance already discussed in this paper, the QDIP array technology offers additional positive attributes that should not be overlooked. Large substrates (150-mm wafers) are readily available for growth. A 150-mm GaAs wafer contains sufficient real estate to produce over forty 640 × 512 arrays at a 25-μm pitch, thus providing favorable economy of scale. Also, since the QDIP FPA thinning technology eliminates thermal mismatching problems, the array area can be quite large. This, coupled with the demonstrated spatial uniformity, makes it feasible to produce very large format (multimega-pixel) QDIP FPAs.

Acknowledgment

The authors are grateful to R. Cox, S. Forouhar, P. Grunthaner, J. Hong, J. Hyon, C. Khan, K. Koliwad, T. Krabach, A. Larson, T. Luchik, R. Odle, C. Ruoff, R. Staehle, and N. Toomarian for encouragement and support during the development and optimization of QDIP FPAs at the Jet Propulsion Laboratory (JPL) for various applications. The authors would like to give their special thanks to Prof. P. Bhattacharya of the University of Michigan for his support during the early days of this work at JPL.

References

[1] V. Ryzhii, "The theory of quantum-dot infrared photodetector," *Semicond. Sci. Technol.*, vol. 11, pp. 759–765, 1996.

[2] J. Phillips, K. Kamath, and P. Bhattacharya, "Far-infrared photoconductivity in self-organized InAs quantum dots," *Appl. Phys. Lett.*, vol. 72, pp. 2020–2022, 1998.

[3] D. Pal, L. Chen, and E. Towe, "Intersublevel photoresponse of (In,Ga)As/GaAs quantum-dot photodetectors: Polarization and temperature dependence," *Appl. Phys. Lett.*, vol. 83, pp. 4634–4636, 2003.

[4] S. Chakrabarti, A. D. Stiff-Roberts, P. Bhattacharya, S. Gunapala, S. Bandara, S. B. Rafol, and S. W. Kennerly, "High-temperature operation of InAs-GaAs quantum-dot infrared photodetectors with large responsivity and detectivity," *IEEE Photon. Technol. Lett.*, vol. 16, no. 5, pp. 1361–1363, May 2004.

[5] E. T. Kim, A. Madhukar, Z. Ye, and J. C. Campbell, "High detectivity InAs quantum dot infrared photodetectors," *Appl. Phys. Lett.*, vol. 84, pp. 3277–3279, 2004.

[6] Z. Ye, J. Campbell, Z. Chen, E. T. Kim, and A. Madhukar, "Noise and photoconductive gain in InAs quantum-dot infrared photodetectors," *Appl. Phys. Lett.*, vol. 83, pp. 1234–1236, 2003.

[7] P. Bhattacharya, X. H. Su, S. Chakrabarti, G. Ariyawansa, and A. G. U. Perera, "Characteristics of a tunneling quantum-dot infrared photodetector operating at room temperature," *Appl. Phys. Lett.*, vol. 86, pp. 191106–191108, 2005.

Authorized licensed use limited to: IEEE Xplore. Downloaded on November 24, 2008 at 11:15 from IEEE Xplore. Restrictions apply.

[8] W. Zhang, H. Lim, M. Taguchi, S. Tsao, B. Movaghar, and M. Razeghi, "High-detectivity InAs quantum-dot infrared photodetectors grown on InP by metal-organic chemical-vapor deposition," *Appl. Phys. Lett.*, vol. 86, pp. 191103–191104, 2005.
[9] V. G. Stoleru and E. Towe, "Oscillator strength for interband transitions in (In, Ga)As/GaAs quantum dots," *Appl. Phys. Lett.*, vol. 83, pp. 5026–5028, 2003.
[10] S. Krishna, "Quantum dots-in-a-well infrared photodetector," *J. Phys. D*, vol. 38, pp. 2142–2150, 2005.
[11] S. Raghavan, P. Rotella, A. Stintz, B. Fuchs, S. Krishna, C. Morath, D. A. Cardimona, and S. W. Kennerly, "High-responsivity, normal incidence long-wave infrared ($\lambda \sim 7.2\ \mu$m) InAs/$In_{0.15}Ga_{0.85}As$ dots-in-a-well detector," *Appl. Phys. Lett.*, vol. 81, pp. 1369–1371, 2002.
[12] J. Jiang, K. Mi, S. Tsao, W. Zhang, H. Lim, T. O'Sullivan, T. Sills, M. Razeghi, G. J. Brown, and M. Z. Tidrow, "Demonstration of a 256×256 middle-wavelength infrared focal plane array based on InGaAs/InGaP quantum dot infrared photodetectors," *Appl. Phys. Lett.*, vol. 84, pp. 2232–2234, 2004.
[13] S. Krishna, D. Forman, S. Annamalai, P. Dowd, P. Varangis, T. Tumolillo, A. Gray, J. Zilko, K. Son, M. Liu, J. Campbell, and D. Carothers, "Demonstration of a 320×256 two-color focal plane array using InAs/InGaAs quantum dots in well detector," *Appl. Phys. Lett.*, vol. 86, pp. 193501–193503, 2005.
[14] I. N. Stranski and L. Krastanow, "Zur Theorie der orientierten Ausscheidung von Ionenkristallen aufeinander," in *Sitzungsberichte d. Akad. D. Wissenschaften in Wien*, Mathnaturwiss, Klasse, 1937, vol. 146, pp. 797–810.
[15] S. Raghavan, D. Forman, P. Hill, N. R. Weisse-Berstein, G. von Winckel, P. Rotella, S. Krishna, S. Kennerly, and J. W. Little, "Normal-incidence InAs/$In_{0.15}Ga_{0.85}As$ quantum dots-in-a-well detector operating in the long-wave infrared atmospheric window (8–12 μm)," *J. Appl. Phys.*, vol. 96, pp. 1036–1039, 2004.
[16] S. D. Gunapala, S. V. Bandara, J. K. Liu, E. M. Luong, S. B. Rafol, J. M. Mumolo, D. Z. Ting, J. J. Bock, M. E. Ressler, M. W. Werner, P. D. LeVan, R. Chehayeb, C. A. Kukkonen, M. Levy, P. LeVan, and M. A. Fauci, "Quantum Well Infrared Photodetector Research and Development at Jet Propulsion Laboratory," *Sens. Mater.*, vol. 12, pp. 327–351, 2000.
[17] S. D. Gunapala and S. V. Bandara, "Quantum Well Infrared Photodetector (QWIP) Focal Plane Arrays," in *Semiconductors and Semimetals*. New York: Academic, 1999, vol. 62, pp. 197–282.
[18] D. Z.-Y. Ting, Y.-C. Chang, S. V. Bandara, C. J. Hill, and S. D. Gunapala, "Band Structure and Impurity Effects on Optical Properties of Quantum Well and Quantum Dot Infrared Photodetectors," in *Infrared Phys. Technol.*, Apr. 2007, to be published.
[19] P. Boucaud and S. Sauvage, "Infrared photodetection with semiconductor self-assembled quantum dots," *C. R. Physique*, vol. 4, pp. 1133–1154, 2003.
[20] S. Krishna, D. Forman, S. Annamalai, P. Dowd, P. Varangis, T. Tumolillo, Jr, A. Gray, J. Zilko, K. Sun, M. Liu, J. Campbell, and D. Carothers, "Demonstration of a 320×256 two-color focal plane array using InAs/InGaAs quantum dots in well detectors," *Appl. Phys. Lett.*, vol. 86, pp. 193501-1–193501-3, 2005.
[21] J. Jiang, K. Mi, S. Tsao, W. Zhang, H. Lim, T. O'Sullivan, T. Sills, M. Razeghi, G. J. Brown, and M. Z. Tidrow, "Demonstration of a 256×256 middle-wavelength infrared focal plane array based on InGaAs/InGaP quantum dot infrared photodetectors," *Appl. Phys. Lett.*, vol. 84, pp. 2232–2234, 2004.
[22] S.-F. Tang, C.-D. Chiang, P.-K. Weng, Y.-T. Gau, J.-J. Luo, S.-T. Yang, C.-C. Shih, S.-Y. Lin, and S.-C. Lee, "High-Temperature Operation Normal Incident 256×256 InAs-GaAs Quantum-Dot Infrared Photodetector Focal Plane Array," *IEEE Photon. Technol. Lett.*, vol. 18, no. 8, pp. 986–988, Apr. 2006.

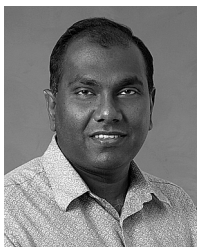

Sarath D. Gunapala received the Ph.D. degree in physics from the University of Pittsburgh, Pittsburgh, PA, in 1986.

Since 1986, he studied infrared properties of III–V compound semiconductor heterostructures and the development of quantum-well infrared photodetectors (QWIPs) for infrared imaging at AT& T Bell Laboratories. He joined NASA's Jet Propulsion Laboratory, California Institute of Technology, Pasadena, in 1992. There he leads the Infrared Focal Planes and Photonics Technology Research Group. He is also a Senior Research Scientist and a Principal Engineer at NASA Jet Propulsion Laboratory. He has authored over 200 publications, including several book chapters on QWIP imaging focal plane arrays, and holds 15 patents.

Sumith V. Bandara received the Ph.D. degree from the University of Pittsburgh, Pittsburgh, PA, in 1989.

Currently, he is a Senior Member of Technical Staff in the Infrared Focal Plane and Phototnic Technology Group, NASA Jet Propulsion Laboratory, Pasadena, CA. He has over ten years of experience in semiconductor devices including quantum-well infrared photodetector (QWIP) research. Prior to joining Jet Propulsion Laboratory, he worked at Bell Laboratories, Murray Hill, NJ, and at the University of Pittsburgh where his work involved new semiconductor device design, theoretical modeling, fabrication, optical coupling, and performance analysis. He has authored and co-authored over 80 technical publications including extensive reviews on QWIPs.

Cory J. Hill received the B.S. degree in physics from the University of Southern California, Los Angeles, in 1996, and the M.S. and Ph.D. degrees in applied physics from the California Institute of Technology, Pasadena, in 1998 and 2001, respectively.

He is currently a Member of the Engineering Staff at the Jet Propulsion Laboratory, Pasadena, CA, in the *In Situ* Technology and Experiments Systems Section. His research activities include device design and molecular beam epitaxial growth of III–V As and Sb-based materials for mid-IR lasers, IR focal plane arrays, and avalanche photodiodes.

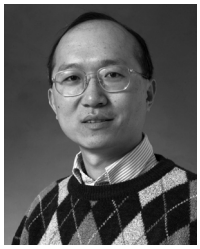

David Z. Ting received the B.S. degree (hons.) in physics from the California Institute of Technology, Pasadena, in 1980, and the M.S. and Ph.D. degrees in physics from the University of Illinois at Urbana-Champaign in 1981 and 1986, respectively.

He was a Senior Research Fellow in the Department of Applied Physics at Caltech before joining the National Tsing Hua University, Hsinchu, Taiwan, R.O.C., as an Associate Professor of Physics in 1995. He is currently a Senior Member of Engineering Staff in the Infrared Photonics Technology Group, Jet Propulsion Laboratory. His research activities include the studies of electronic, optical, and thermoelectric properties of semiconductor alloys, superlattices, quantum wells, wires, and dots, modeling of heterostructure infrared detectors and lasers, quantum transport in tunnel devices and nanostructure, optical simulations, nanophotonic devices, and spintronics. Results of his work have been reported in over 130 research publications and in over 100 conference presentations and technical seminars.

Dr. Ting is a member of the American Physical Society, the Materials Research Society, and the IEEE Lasers and Electro-Optics Society.

John K. Liu received the B.S. degree in engineering science and bioengineering from the University of California, San Diego, in 1984, and the M.S.E.E. from California State University, Los Angeles, in 1986.

During 1985-1989, he worked at the Jet Propulsion Laboratory (JPL), Pasadena, on solar cell and III–V molecular beam epitaxy (MBE) growth. During 1989-1991, he worked at TRW on III–V thin film growth using MBE for MMIC applications. Since 1991, he has been working on the development of QWIP IR camera at JPL. His current interests are in QWIP FPA fabrications and characterizations.

Authorized licensed use limited to: IEEE Xplore. Downloaded on November 24, 2008 at 11:15 from IEEE Xplore. Restrictions apply.

Sir B. Rafol received the B.E.E.T. degree from DeVry Institute of Technology, Chicago, IL, in 1976, the M.A. degree in physics degree from Kent State University, Kent, OH, in 1982, and the Ph.D. degree in physics from University of Illinois, Chicago, in 1991.

He joined USRobotics, Mount Prospect, IL, in 1995, and Rockwell, Woods Dale, IL, in 1997, where he worked on telecommunication systems. In 1998, he joined Jet Propulsion Laboratory, California Institute of Technology, Pasadena, where he has been working on characterization of QWIP focal plane array, detector development, and system testing. His research interest is on transport properties of low dimensional quantum systems and quantum detectors.

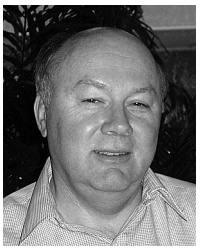

Edward R. Blazejewski received the Ph.D. from American University, Washington, DC, in 1980.

He is currently a Senior Member of the Technical Staff in the Space Experiments Systems Section, Jet Propulsion Laboratory (JPL), Pasadena, CA. He has over 30 years experience in the area of visible and infrared imaging device development. Prior to joining JPL, he was involved in thin film and MIS sensor development at the Night Vision Laboratory, Ft. Belvior. He has held key management positions at both Santa Barabara Research Center and the Rockwell International Science Center in the area of intrinsic heterostructure IR focal plane array development and at EMagin Corporation in the area of field emission flat panel array development. He has authored and co-authored over 50 technical publications.

Jason M. Mumolo received the B.S. degree in electrical engineering from the Polytechnic University of California, Pomona, in 2001.

He joined the Jet Propulsion Laboratory, California Institute of Technology, Pasadena, in 1997 as an undergraduate part-time student. Upon graduating, he joined the Infrared Focal Planes and Photonics Technology Group under S. Gunapala as a Process Engineer. His current work and interest is in the development and fabrication of QWIP devices and focal plane arrays for camera systems.

Sam A. Keo received the B.S. degree in engineering technology from the Polytechnic University of California, Pomona, in 1999.

During 1987–1989, he worked at Ortel Corporation on semiconductor laser fabrication. From 1989 to 1991, he worked at Rockwell International on photonic devices. In 1991–1999, worked at the Jet Propulsion Laboratory (JPL), Pasadena, on the development of semiconductor lasers for space applications. During 1999–2003,he worked at Genoa Inc., Lightcross Inc., and ModeTek Inc., on telecom devices. Since 2003, he has been working on the development of QWIP IR detectors at JPL. His current work and interest is in the development and fabrication of QWIP devices and focal plane arrays for camera systems.

Sanjay Krishna received the M.S. degree in physics from the Indian Institute of Technology, Madras, India, in 1996, the M.S. in electrical engineering and the Ph.D. degree in applied physics from the University of Michigan, Ann Arbor, in 1999 and 2001, respectively.

He is an Associate Professor of Electrical and Computer Engineering at the Center for High Technology Materials at University of New Mexico, Albuquerque. He joined the University of New Mexico as a tenure track faculty member in 2001. He has authored/co-authored more than 40 peer-reviewed journal articles, over 40 conference presentations, two book chapters, and has four provisional patents.

Dr. Krishna has also served as the chair of the local IEEE LEOS chapter.

Y.-C. Chang received the Ph.D. degree in physics from California Institute of Technology, Pasadena, in 1980.

In September 1980, he joined the Physics Department of University of Illinois at Urbana-Champaign, where he is currently a Professor. He has more than 20 years experience in theoretical studies of electronic, vibrational, optical, and transport properties of nanoscale heterostructures, including various kinds of quantum-well, quantum-wire, and quantum-dot systems. Over the years, he has worked as summer faculty or consultant at numerous government and industrial labs, including Sandia National Laboratory, Brookhaven National Laboratory, Jet Propulsion Laboratory, IBM Research Center, Bell Communications, Rockwell Science Center, Hughes Research Laboratory, Honeywell Science Center, and Thermawave Inc. He has published more than 250 papers in refereed journals. He is listed as "highly cited scientist" by ISI highlycited.com.

Dr. Chang is the recipient of the Dr. C. S. Wu scholarship in 1972 and 1973. He was elected as Fellow of American Physical Society in 2001. He has been awarded "Distinguished Visiting Scientist" at Jet Propulsion Laboratory for 2004–2006.

Craig A. Shott received the B.S. degree in earth science from the University of California in 1985, and pursued graduate coursework in solid state electrical engineering at the University of California Santa Barbara.

He is currently Manager of the Microbolometer Production group at FLIR Systems, Goleta, CA. He has 19 years of experience in process engineering of HgCdTe, InSb, QWIP, and Microbolometer devices.

Authorized licensed use limited to: IEEE Xplore. Downloaded on November 24, 2008 at 11:15 from IEEE Xplore. Restrictions apply.